ISSN 0036-0295, Russian Metallurgy (Metally), Vol. 2020, No. 6, pp. 640–648. © Pleiades Publishing, Ltd., 2020.
Russian Text © The Author(s), 2019, published in Elektrometallurgiya, 2019, No. 12, pp. 9–18.

THEORY OF METALLURGICAL PROCESSES

Phase Equilibria in the Liquid Steel Deoxidized with Aluminum and Calcium in the Presence of Magnesium

G. G. Mikhailov[a], *, L. A. Makrovetz[a], O. V. Samoilova[a], and L. A. Smirnov[b]

[a] *National Research University Southern-Ural State University, Chelyabinsk, 454080 Russia*

[b] *Institute of Metallurgy, Ural Branch, Russian Academy of Sciences, Yekaterinburg, 620016 Russia*

**e-mail: mikhailovgg@susu.ru*

Received June 14, 2019; revised August 20, 2019; accepted August 23, 2019

Abstract—The concentration regions of the phase equilibria of the components in a metallic Fe–Mg–Al–Ca–C–O melt at a temperature of 1600°C have been calculated and built for low-, medium-, and high-carbon steels by simulating the solubility surfaces of the components in a metal. The conditions of formation of calcium aluminate inclusions in the system are determined. Carbon is shown to influence the sequence of phase formation with the participation of strong deoxidizers, such as calcium, magnesium, and aluminum. The liquid metal is found to contain composition regions in equilibrium with a gaseous CO-based phase or a gaseous phase based on calcium and magnesium vapors.

Keywords: deoxidation, phase equilibria, Fe–Mg–Al–Ca–C–O system, simulation, solubility surface

DOI: 10.1134/S0036029520060130

INTRODUCTION

Deoxidation is the most important operation of a metallurgical technology that enables one to ensure, to a significant degree, the quality of a melted metal by the formation of the rational composition of nonmetallic inclusions and by a decrease in the oxidation level of the metal. One of the most commonly used deoxidizers of iron-based melts is aluminum due to its comparable availability, the possibility of forming a deeply deoxidized metal, and positive influence on the initial grain size [1–3]. Calcium is also widely used as a deoxidizing and desulfurizing agent and for the modification of nonmetallic inclusions due to its high chemical activity with respect to oxygen and sulfur in liquid iron [4–7]. The application of aluminum–calcium alloys for the deoxidation of complex alloys makes it possible not only to provide a large deoxidation depth, but also to reach a globular shape of nonmetallic inclusions [8–12].

During production, a liquid metal contacts with the magnesia refractory material of the liner of steelmaking units and ladles and a magnesium-containing slag, which can change the nature of the deoxidizing action of aluminum–calcium combinations. In some technological processes, special magnesium-containing deoxidizing complexes are used [13, 14].

The aim of this work is to perform thermodynamic simulation of the phase equilibria in an Fe–Mg–Al–Ca–C–O melt at a temperature of 1600°C for low-, medium-, and high-carbon steels.

SIMULATION PROCEDURE

In this work, the thermodynamic simulation was performed using the technique of constructing the solubility surfaces of metal components (SSMC) [15]. The solubility surface of metal components relates quantitative changes in the liquid metal compositions to changes in the nonmetallic inclusion compositions, which enables one to calculate the concentration regions of the thermodynamic stability of the nonmetallic phases existing in equilibrium with a metallic melt.

The SSMC coordinates of the Fe–Mg–Al–Ca–C–O system were calculated taking into account the data on the limiting solubility of elements in liquid iron at 1600°C: the oxygen solubility is 0.23 wt % [15], the magnesium solubility is 0.02 wt % [16], and the calcium solubility is 0.0463 wt % [17].

To determine possible chemical reactions in the melt of the system and the nonmetallic inclusion compositions, we performed SSMC calculations considering the following phase equilibria that take place in oxide systems: FeO–MgO, FeO–Al_2O_3, FeO–CaO, Al_2O_3–CaO, MgO–Al_2O_3, MgO–CaO, and FeO–MgO–Al_2O_3–CaO. In this case, we used the available data, according to which the melting temperature of iron oxide FeO is 1378°C [18], that of magnesium oxide MgO is 2825°C [18], that of aluminum oxide Al_2O_3 is 2051°C [18], and that of calcium oxide CaO is 2613°C [19].

Table 1. Temperature dependences for the equilibrium constants of the reactions that occur in the metallic melt of the system under study [23–25]

Chemical reaction	$\log K = A/T + B$	
	A	B
(FeO) = [Fe] + [O]	–6320	+4.734
(MgO) = [Mg] + [O]	–22457	+6.545
(Al_2O_3) = 2[Al] + 3[O]	–58383	+18.063
(CaO) = [Ca] + [O]	–31368	+12.515
$\|FeO\|_{s.s}$ = [Fe] + [O]	–8069	+5.800
$\|MgO\|_{s.s}$ = [Mg] + [O]	–26500	+7.850
$\|Al_2O_3\|$ = 2[Al] + 3[O]	–64000	+20.480
$\|CaO_{s.s}\|$ = [Ca] + [O]	–34100	+13.460
$\|FeAl_2O_4\|_{s.s}$ = [Fe] + 2[Al] + 4[O]	–76069	+27.365
$\|MgAl_2O_4\|_{s.s}$ = [Mg] + 2[Al] + 4[O]	–91239	+27.940
$\|CaAl_{12}O_{19}\|$ = [Ca] + 12[Al] + 19[O]	–426453	+138.178
$\|CaAl_4O_7\|$ = [Ca] + 4[Al] + 7[O]	–161795	+52.367
$\|CaAl_2O_4\|$ = [Ca] + 2[Al] + 4[O]	–95258	+31.064
{CO} = [C] + [O]	–1168	–2.070
$\{CO_2\}$ = [C] + 2[O]	–9616	+2.510
{Mg} = [Mg]	+6670	–6.480
{Ca} = [Ca]	+1912	–2.700

* In parentheses, oxide melt components are given; in brackets, metallic melt components; in straight brackets, solid compounds; and in curly brackets, gaseous phases.

The FeO–MgO phase diagram is characterized by unlimited solubility of the components in both solid and liquid states [20]. The data on the binary oxide phase diagrams for the FeO–Al_2O_3, MgO–Al_2O_3, FeO–CaO, Al_2O_3–CaO, and MgO–CaO systems were taken from [21]. For example, in the FeO–Al_2O_3 system, hercynite $FeAl_2O_4$ with a melting temperature of 1780°C can form. In the MgO–Al_2O_3 system, a magnesium oxide-based solid solution forms along with the formation of magnesia spinel $MgAl_2O_4$, with a melting temperature of 2105°C. The solubility of Al_2O_3 in MgO at 1600°C is lower than 0.5 wt %, which determined the possibility of SSMC calculation without considering the solubility of aluminum oxide in MgO. In the FeO–CaO system, there are solid solutions based on iron oxide and calcium oxide. The existence of two solid solutions is also confirmed in the MgO–CaO system with the minimum solubility of calcium oxide in MgO at 1600°C, which enables us to calculate SSMC without considering the formation of this solid solution. The Al_2O_3–CaO system does not contain solid solutions; however, there are the following four compounds observed experimentally: $CaAl_{12}O_{19}$ (T_m = 1830°C), $CaAl_4O_7$ (T_m = 1762°C), $CaAl_2O_4$ (T_m = 1602°C), and $Ca_3Al_2O_6$ (T_m = 1539°C).

The FeO–MgO–Al_2O_3–CaO phase diagram in poorly described. Handbook [21] gives data only on the total projection of the liquidus surface in the FeO–Al_2O_3–CaO and MgO–Al_2O_3–CaO systems; for the FeO–MgO–Al_2O_3, the positions of isotherms are shown for temperatures 1400 and 1700°C; it is found that the MgO–Al_2O_3–CaO system contains the ternary $Ca_3MgAl_4O_{10}$ compound, whch exists to 1500°C. Only a continuous series of solid solutions was detected in the pseudo-binary $FeAl_2O_4$–$MgAl_2O_4$ system [22].

Thus, at 1600°C, which is characteristic of steelmaking processes, the following phases can form in the Fe–Mg–Al–Ca–C–O system as reaction products: an oxide variable-composition melt (FeO, MgO, Al_2O_3, CaO); solid solution $|FeO, MgO|_{s.s.}$; corundum Al_2O_3; solid solution of spinels $|FeAl_2O_4, MgAl_2O_4|_{s.s.}$; calcium oxide-based solid solution $|CaO|_{s.s.}$; calcium aluminates $CaAl_{12}O_{19}$, $CaAl_4O_7$, and $CaAl_2O_4$; and gaseous reaction products {CO, CO_2}, which also contain magnesium and calcium vapors. The temperature dependences of the equilibrium constants of the reactions of formation of these phases in the metallic melt of the system under study are given in Table 1.

Table 2. Energy parameters Q_{ijkl} of the theory of subregular ionic solutions for an oxide melt

System	Q_{ijkl}, J/mol		
FeO–MgO	−5000	−25000	−15000
FeO–Al_2O_3	+212	−21502	−11091
MgO–Al_2O_3	−35361	−64760	+8618
FeO–CaO	−25767	−56788	−26522
MgO–CaO	+34913	+23919	+31326
Al_2O_3–CaO	−97668	−172657	−51474
FeO–MgO–Al_2O_3	−50915	−103336	−56854
FeO–MgO–CaO	−49122	−7897	−22881
FeO–Al_2O_3–CaO	−145150	−233108	−200814
MgO–Al_2O_3–CaO	−300000	−300000	−200000

Table 3. Energy parameters Q_{ijkl} of the theory of subregular ionic solutions for calculating the activities of the CaO-based solid solution components

System	Q_{ijkl}, J/mol		
FeO–CaO	+33362	+66724	+33362
MgO–CaO	+52869	+105738	+52869
FeO–MgO–CaO	+125593	+175462	+145100

The simulation of the phase equilibria with the participation of an oxide melt and/or the solid solutions of $|CaO|_{s.s.}$ oxides was performed using the theory of subregular ionic solutions, the energy parameters of which are given in Tables 2 and 3. The activities of the components of the $|FeO, MgO|_{s.s.}$ solid solution were calculated using the theory of regular ionic solutions; in this case, we found that the theory energy parameter was $Q_{12} = +3000$ J/mol. The $|FeAl_2O_4, MgAl_2O_4|_{s.s.}$ solutions were considered to be completely ionic. The metallic melt was modeled using the Wagner first-order interaction parameters (Table 4). The activities of pure solid-state aluminum oxide and calcium aluminates were taken to be 1. The activities of the gaseous phase components were determined via their partial pressures.

The simulation was performed for the following four carbon concentrations in steel: 0 wt % (equilibria for the deoxidation of pure iron), 0.1 wt % (characteristic of low-carbon steel), 0.4 wt % (medium-carbon steel), and 0.8 wt % (high-carbon steel). The limits of the Mg, Al, and Ca concentrations were as follows: for magnesium, from 10^{-6} wt %; for calcium, from 10^{-5} wt % to the limiting solubility in liquid iron; and for aluminum, from 10^{-5} to 0.1 wt %.

RESULTS AND DISCUSSIONS

The results of simulating the isocompositional SSMC sections of the Fe–Mg–Al–Ca–C–O system at $T = 1600$°C are shown in Figs. 1–4. All the diagrams were plotted in log–log coordinates and the concentrations are given in wt %. In each case, the concentration of one element of the system, which is characteristic of steelmaking was fixed: in Figs. 1 and 2, magnesium concentrations of 0.0001 and 0.0005 wt % were fixed, respectively; Fig. 3 shows the data calculated at a calcium content of 0.001 wt % in liquid metal; and Fig. 4 shows the results of simulation at [Al] = 0.01 wt %.

In Figs. 1–4, region I indicates the compositions of the liquid metal in equilibrium with the inclusions of the $|FeO, MgO|_{s.s}$ solid solution; in region II, $|FeAl_2O_4, MgAl_2O_4|_{s.s}$ spinel solid solution inclusions are the nonmetallic inclusions in equilibrium with the liquid metal, which are thermodynamically stable; in region III, corundum inclusions are in equilibrium with the liquid metal; in regions IV and V, the inclusions of calcium hexa- and bialuminates, respectively; in region VI, the liquid metal compositions in equilibrium with an oxide melt of variable compositions

Table 4. First-order interaction parameters of liquid iron components e_i^j (1600°C)

i	j				
	Mg	Al	O	C	Ca
Mg	0 [26, 27]	−0.017 [26, 28]	−3 [29, 30]	+0.15 [32]	−0.062 [33]
Al	−0.0195 [26, 28]	+0.045 [27]	−1.98 [27]	+0.091 [32]	−0.047 [32]
O	−1.98 [29]	−1.17 [31]	−0.2 [27, 30]	−0.45 [32]	−1.41 [24]
C	+0.07 [32]	+0.043 [32]	−0.34 [32]	+0.14 [32]	−0.097 [32]
Ca	−0.102 [33]	−0.072 [32]	−3.62 [24]	−0.34 [32]	−0.002 [32]

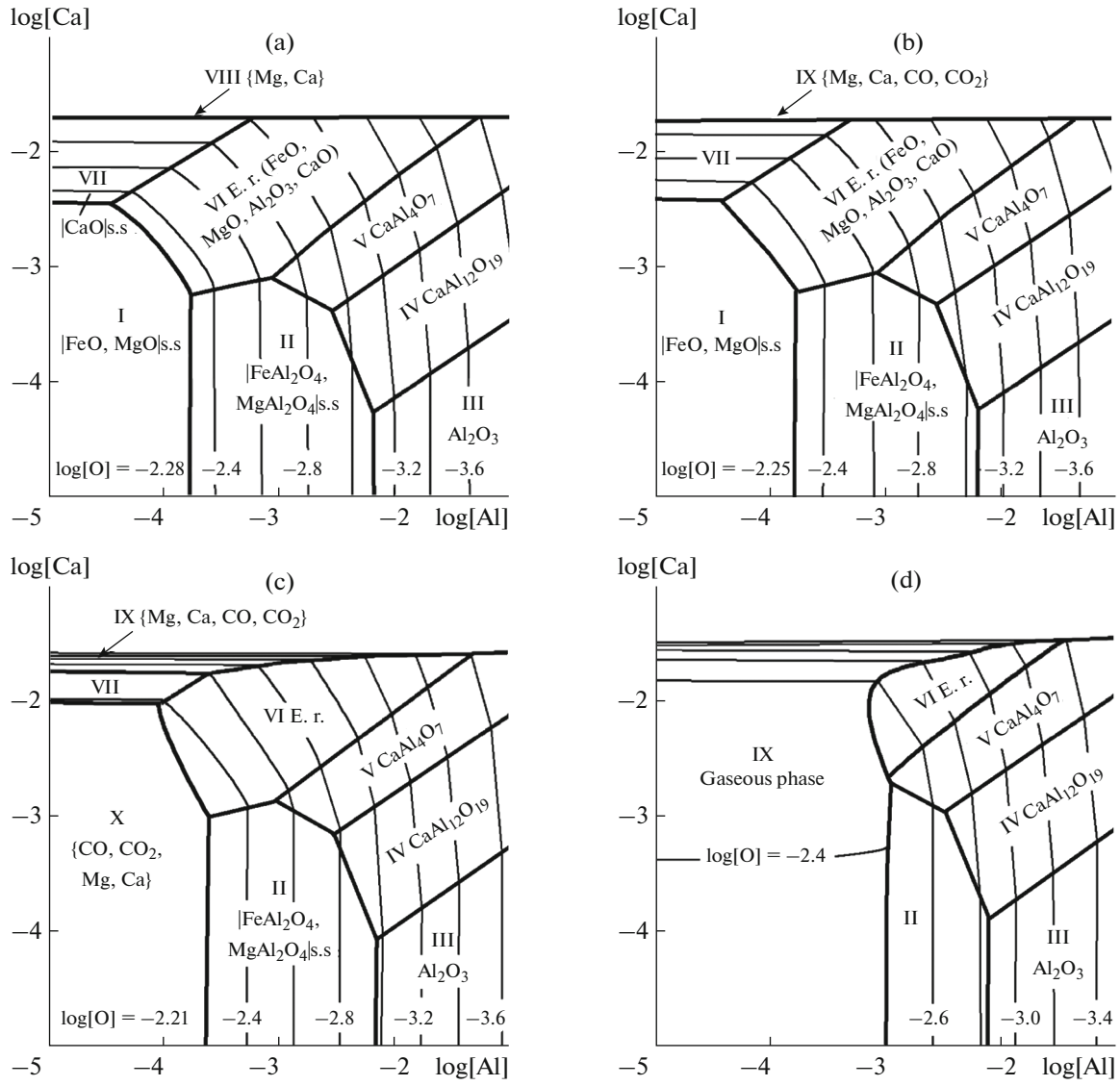

Fig. 1. SSMCs of the Fe–Mg–Ca–Al–O–C system, [Mg] = 0.0001 wt % and [C] = (a) 0, (b) 0.1, (c) 0.4, and (d) 0.8 wt %.

(FeO, MgO, Al_2O_3, CaO) are given; in region VII, in equilibrium with calcium oxide-based $|CaO|_{s.s}$ solid solution; in region VIII, in equilibrium with a gaseous phase consisted of {Mg, Ca} vapors; in region IX, in equilibrium with a gaseous {Mg, Ca, CO, CO_2} phase with a predominance of magnesium and calcium vapors in the composition; in region X, in equilibrium with a gaseous {CO, CO_2, Mg, Ca} phase with a predominance of carbon monoxide in the composition; and in region XI, in equilibrium with a gaseous variable-composition phase. Table 5 gives the calculated gas phase compositions (total pressure in the system was P_{tot} = 1.013 MPa).

The available data for the Fe–Mg–Al–Ca–C–O system are contradictory and restricted. In [34], experimental results on the determination of the phase compositions of the nonmetallic inclusions formed at [Mg] = 0.0005 wt % and [C] = 0 wt % are presented (points in Fig. 2a); according to these data, the metal contains spinel inclusions (with the predominance of $MgAl_2O_4$ in the solution composition), which agrees with the results of our simulation. On the other hand, according to the calculated data in [35], magnesium oxide cannot be in equilibrium with the liquid metal at such magnesium and carbon concentrations, but this fact does not correspond to both our calculation results and the conclusions in [34].

As follows from Figs. 1–4, an increase in the carbon concentration (other things being equal) leads to a decrease in the probability of forming liquid oxide nonmetallic inclusions.

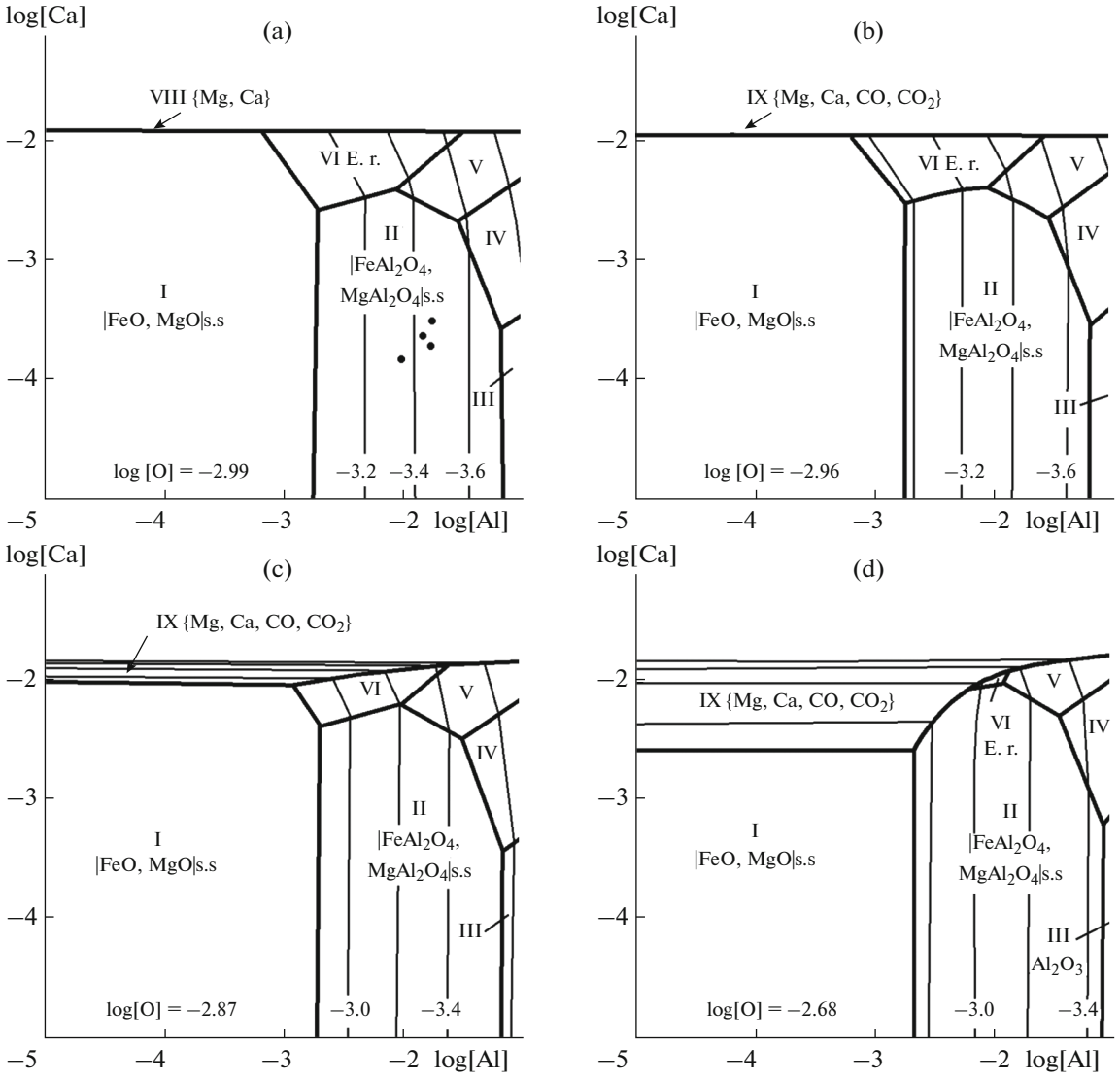

Fig. 2. SSMCs of the Fe–Mg–Ca–Al–O–C system, [Mg] = 0.0005 wt % and [C] = (a) 0, (b) 0.1, (c) 0.4, and (d) 0.8 wt %. Points denote the experimental results [34] corresponding to the region of equilibrium of a liquid metal with a spinel solid solution.

At a magnesium concentration [Mg] = 0.0001 wt % and carbon concentration [C] = 0 and 0.1 wt % (Figs. 1a, 1b), the formation of the carbon monoxide gaseous phase is thermodynamically unlikely, and there is no region X. A similar regularity can also be observed at a calcium concentration [Ca] = 0.001 wt % (Figs. 3a, 3b). The region of the liquid metal compositions in equilibrium with a carbon monooxide-based gaseous phase disappears for all fixed carbon concentrations at a magnesium concentration of 0.0005 wt % in steel (Fig. 2) or an aluminum concentration of 0.01 wt % (Fig. 4). On the other hand, the results of the calculations based the equilibrium oxygen concentration in regions X and XI in Figs. 1c, 1d, 3c, and 3d are comparable with the data for the Fe–C–O system [36], according to which the equilibrium oxygen concentration in steel is 0.00625 wt % (log[O] = –2.20) at [C] = 0.4 wt % and [O] = 0.003125 wt % (log[O] = –2.51) at [C] = 0.8 wt %. According to our data, the equilibrium oxygen concentration in region X in Figs. 1c and 3c ([C] = 0.4 wt %) is 0.00617 wt % (log[O] = –2.21); at a carbon concentration of 0.8 wt % in regions X (Fig. 3d) and XI (Fig. 1d), the calculated equilibrium oxygen concentration is 0.003981 wt % (log[O] = –2.4).

Analyzing Figs. 1 and 2, we can note that an increase in the magnesium concentration in the steel, all other conditions being equal, decreases the possibility of participation of carbon in the deoxidation process. For example, at [Mg] = 0.0001 wt % and [C] = 0.8 wt % (Fig. 1d), condensed or liquid deoxidation products can form only from an aluminum con-

Table 5. Results of calculating the gaseous phase compositions in the pressure range (MPa) in the Fe–Mg–Ca–Al–O–C system

Fig. no	Equilibrium region	$p_{\{CO\}}$	$p_{\{CO_2\}} \times 10^4$	$p_{\{Mg\}}$	$p_{\{Ca\}}$
1a	VIII	–	–	0.0833–0.0834	0.9293–0.9300
1b	IX	0.0047–0.0506	0.003–4.05	0.0860–0.0863	0.8766–0.9223
1c	IX	0.0198–0.3309	0.011–4.05	0.0947–0.0957	0.5872–0.8978
	X	0.5759–0.9173	12.16–31.41	0.0925–0.0937	0.0003–0.3423
1d	XI	0.0431–0.9039	0.003–1.32	0.1078–0.1096	0.0002–0.8606
2a	VIII	–	–	0.4165–0.4176	0.5957–0.5967
2b	IX	0.0001–0.0504	0.010–0.40	0.4309–0.4322	0.5319–0.5810
2c	IX	0.0002–0.2006	0.020–1.01	0.4773–0.4790	0.3352–0.5240
2d	IX	0.0004–0.3988	0.040–2.03	0.5471–0.5494	0.0671–0.4635
3a	VIII	–	–	0.9661–0.9668	0.0464–0.0471
3b	IX	0.0062–0.0230	0.006–0.091	0.9467–0.9641	0.0430–0.0436
3c	IX	0.0264–0.1106	0.020–0.507	0.8682–0.9529	0.0339–0.0343
	X	0.8683–0.9673	28.37–35.46	0.0096–0.1092	0.0327–0.0329
3d	IX	0.0581–0.3338	0.051–2.03	0.6543–0.9305	0.0248–0.0249
	X	0.6556–0.9862	7.09–16.21	0.0011–0.3323	0.0244–0.0246
4a	VIII	–	–	0.0083–1.0127	0.0005–1.0049
4b	IX	0.0144–0.0177	0.030–0.051	0.0086–0.9951	0.0004–0.9902
4c	IX	0.0625–0.0767	0.101–0.203	0.0096–0.9362	0.0003–0.9412
4d	IX	0.1405–0.1718	0.304–0.507	0.0109–0.8411	0.0030–0.8618

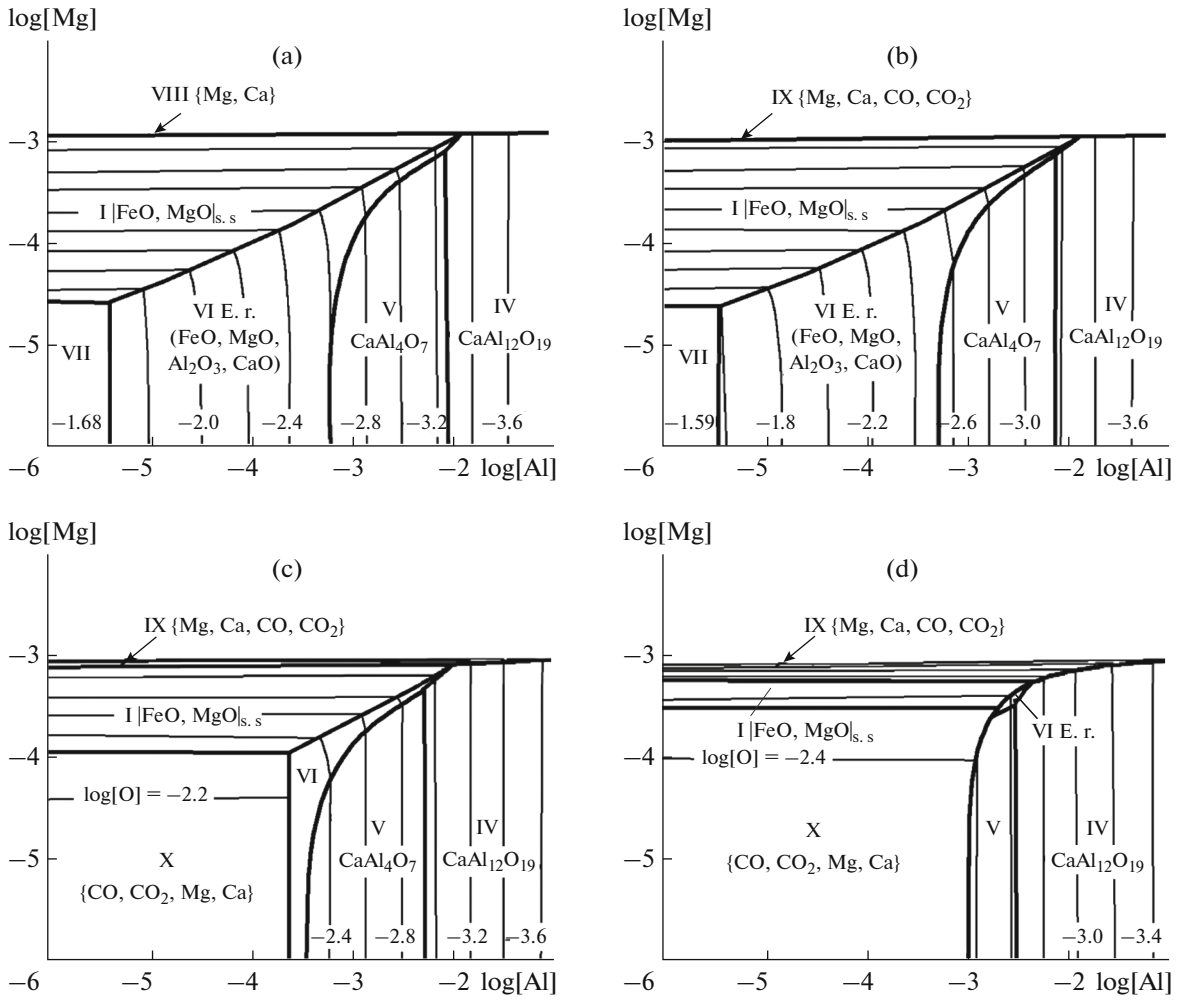

Fig. 3. SSMCs of the Fe–Mg–Ca–Al–O–C system, [Ca] = 0.001 wt % and [C] = (a) 0, (b) 0.1, (c) 0.4, and (d) 0.8 wt %.

centration of 10^{-3} wt %; at a magnesium concentration of 0.0005 wt % and a carbon concentration of 0.8 wt % (Fig. 2d), the region of equilibrium with the carbon monoxide-based gaseous phase disappears, and gaseous phase IX (with the predominance of magnesium and calcium in the composition) is in equilibrium with liquid iron only at the maximum (close to the solubility limit) calcium concentrations.

An increase in the magnesium concentration in the liquid steel under the same conditions (Fig. 2) favors the formation of deoxidation products, such as unfavorable inclusions of oxide solid solutions (with the predominance of MgO in the composition) and spinel solid solutions $[FeAl_2O_4, MgAl_2O_4]_{s.s}$ with the predominance of magnesia spinel in the composition.

At the same time, if the calcium concentration in the liquid steel is 0.001 wt % (Fig. 3), then, according to the performed simulation, the formation of spinel solid solution inclusions is highly impossible thermodynamically, and the formation of particles of oxide solid solution $|FeO, MgO|_{s.s}$ is possible only at magnesium concentrations higher than 10^{-4} wt %. For all fixed carbon concentrations at a given calcium content in the liquid steel, the formation of unfavorable corundum inclusions is highly impossible; however, to form favorable calcium aluminate inclusions, aluminum concentrations higher than 10^{-3} wt % are necessary.

At an aluminum concentration [Al] = 0.01 wt % in the liquid steel (Fig. 4), the equilibrium region with a gaseous phase based on magnesium and calcium vapors is reduced to the solubility limits of Mg and Ca in liquid iron, and carbon is not participated in the deoxidation process. At this aluminum concentration and at the magnesium concentrations not higher than 10^{-4} wt %, calcium aluminate particles should form in the liquid metal as the calcium concentration increases (beginning from ~0.0001 wt % Ca).

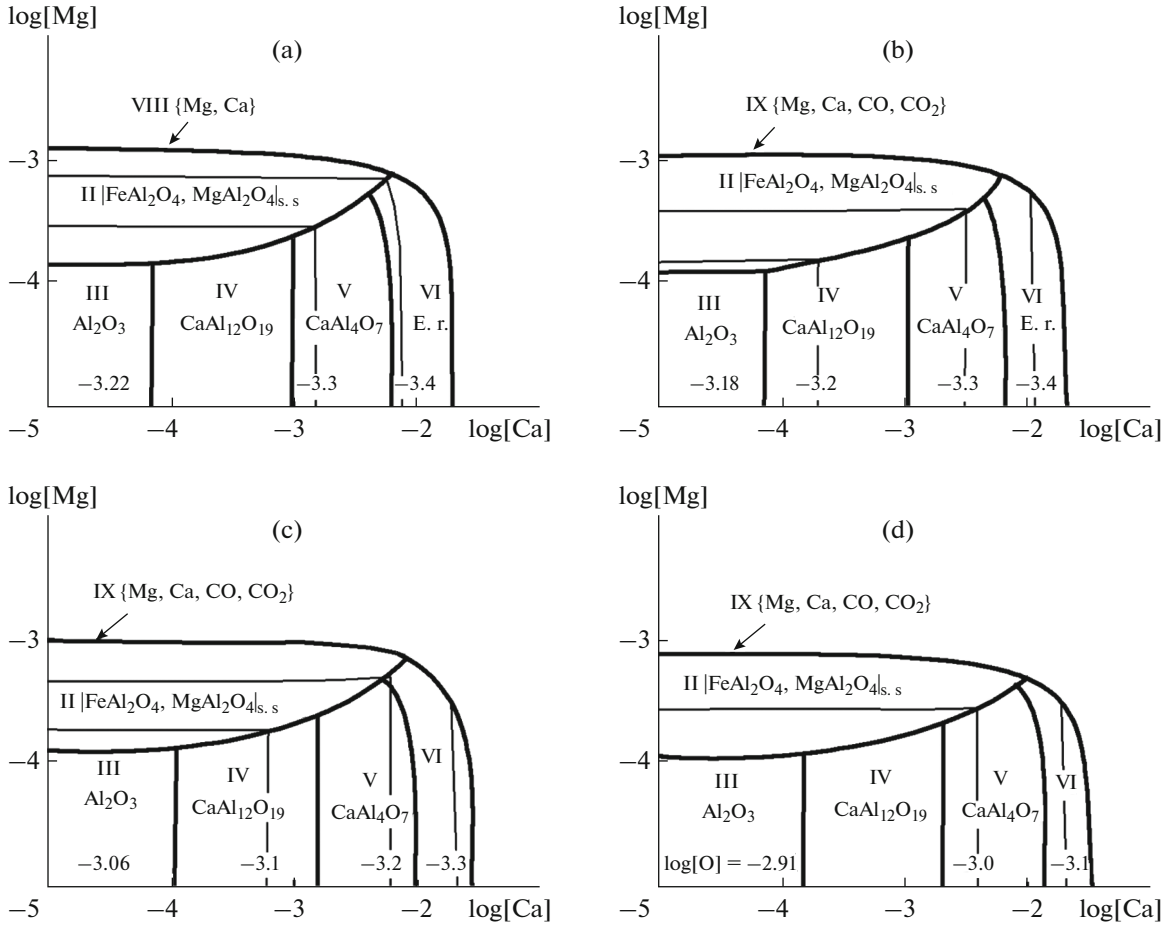

Fig. 4. SSMCs of the Fe–Mg–Ca–Al–O–C system, [Al] = 0.01 wt % and [C] = (a) 0, (b) 0.1, (c) 0.4, and (d) 0.8 wt %.

CONCLUSIONS

We studied the phase equilibria establishing when aluminocalcium master alloys are introduced in the presence of magnesium. A thermodynamic simulation of the phase equilibria in the Fe–Mg–Al–Ca–C–O system at a temperature of 1600°C was performed for the carbon concentrations corresponding to low-, medium, and high-carbon steels. We determined the conditions of the formation of unfavorable nonmetallic inclusions, namely, oxide solid solutions with the predominance of MgO and spinel solid solutions with the predominance of $MgAl_2O_4$ in the composition, in this system. The regions of the phase equilibria in the liquid steel with favorable nonmetallic inclusions of calcium aluminates were also determined. For these inclusions to form, the aluminum concentration in the liquid metal should be about 0.01 wt %, the calcium concentration should be not less than 0.001 wt %, and the magnesium concentration should be controlled at a level of 0.0001 wt %. When the carbon concentration increases, the region of the liquid metal compositions in equilibrium with liquid oxide nonmetallic inclusions narrows and the oxygen concentration increases insignificantly due to a decrease in the activity coefficient (influence of the interaction parameters).

FUNDING

This work was supported by the Government of the Russian Federation (decision no. 211 of March 16, 2013), agreement no. 02.A03.21.0011.

REFERENCES

1. N. A. Gokcen and J. Chipman, “Aluminum–oxygen equilibrium in liquid iron,” Trans. AIME **197**, 173–178 (1953).
2. D. Janke and W. A. Fischer, “Desoxidationsgleichgewichte von titan, aluminum und zirconium in eisenschmelzen bei 1600°C,” Arch. Eisenhüttenwes **47** (4), 195–198 (1976).
3. M. K. Paek, J. M. Jang, Y. B. Kang, et al., “Aluminum deoxidation equilibria in liquid iron: part I. Experimental,” Metall. Mater. Trans. B. **46** (4), 1826–1836 (2015). https://doi.org/10.1007/s11663-015-0368-0

4. K. Mineura, I. Takahashi, and K. Tanaka, "Deoxidation and desulfurization of pressurized liquid high nitrogen stainless steels with calcium," ISIJ Intern. **30** (3), 192–198 (1990). https://doi.org/10.2355/isijinternational.30.192
5. K. Taguchi, H. Ono-Nakazato, D. Nakai, et al., "Deoxidation and desulfurization equilibria of liquid iron by calcium," ISIJ Intern. **43** (11), 1705–1709 (2003). https://doi.org/10.2355/isijinternational.43.1705
6. H. Fujiwara, M. Tano, K. Yamamoto, et al., "Solubility and activity of calcium in molten iron in equilibrium with lime and thermodynamics of calcium containing iron melts." ISIJ Intern. **35** (9), 1063–1071 (1995). https://doi.org/10.2355/isijinternational.35.1063
7. M. Imagumbai and T. Takeda, "Influence of calcium treatment on sulfide- and oxide-inclusions in continuous-cast slab of clean steel—dendrite structure and inclusions," ISIJ Intern. **34** (7), 574–583 (1994). https://doi.org/10.2355/isijinternational.34.574
8. K. Taguchi, H. Ono-Nakazato, T. Usui, et al., "Complex deoxidation equilibria of molten iron by aluminum and calcium, ISIJ Intern. **45** (11), 1572–1576 (2005). https://doi.org/10.2355/isijinternational.45.1572
9. Y. Higuchi, M. Numata, S. Fukagawa, et al., "Inclusion modification by calcium treatment," ISIJ Intern. **36** (S), S151–S154 (1996). https://doi.org/10.2355/isijinternational.36.Suppl_S151
10. G. M. Faulring and S. Ramalingam, "Inclusion precipitation diagram for the Fe–O–Ca–Al system," Metall. Trans. B. **11** (1), 125–130 (1980). https://doi.org/10.1007/BF02657.181
11. E. Kh. Shakhpazov, A. I. Zaitsev, N. G. Shaposhnikov, I. G. Rodionova, and N. A. Rybkin, "Physicochemical prediction of the types of nonmetallic inclusions. Complex deoxidation of steel with aluminum and calcium," Russ. Metall. (Metally), No. 2, 99–107 (2006).
12. A. B. Akhmetov, G. D. Kusainova, A. A. Kuszhanova, et al., "Effect of calcium modification on the Hadfield steel structure and the morphology of nonmetallic inclusions formed in it," Elektrometallurgiya, No. 3, 8–12 (2017).
13. V. I. Zhalybin and G. S. Ershov, "On recovery of liner magnesium during smelting aluminum-alloyed steel," Izv. Akad. Nauk SSSR, Ser. Met., No. 1, 49–53 (1966).
14. V. I. Zhuchkov, S. V. Lukin, and I. V. Shilina, "Deoxidation of steel with calcium–magnesium–silicon ferroalloys," Izv. Vyssh. Uchebn. Zaved., Chern. Met., No. 12, 69–71 (1977).
15. G. G. Mikhailov, B. I. Leonovich, and Yu. S. Kuznetsov, *Thermodynamics of Metallurgical Processes and System*s (MISiS, Moscow, 2009).
16. Y. Du, J. R. Zhao, C. Zhang, et al., "Thermodynamic simulation in the Fe–Mg–Si System," J. Min. Metall. Sect. B. **43** (1), 39–56 (2007). https://doi.org/10.2298/JMMBo701039D
17. M. Berg, J. Lee, and D. Sichen, "Study on the equilibrium between liquid iron and calcium vapor," Metall. Mater. Trans. B. **48** (3), 1715–1720 (2017). https://doi.org/10.1007/s11663-017-0946-4
18. O. Kubaschewski and C. B. Alcock, *Metallurgical Thermochemistr*y (Pergamon, Oxford, 1979).
19. H. A. Wriedt, "The Ca–O (calcium–oxygen) system," Bull. Alloy Phase Diagr. **6** (4), 337–342 (1985). https://doi.org/10.1007/BF02880517
20. P. Wu, G. Eriksson, A. D. Pelton, et al., "Prediction of the thermodynamic properties and phase diagrams of silicate systems: evaluation of the FeO–MgO–SiO_2 system," ISIJ Intern. **33** (1), 26–35 (1993). https://doi.org/10.2355/isijinternational.33.26
21. *Slag Atla*s, Ed. by V. D. Eisenhüttenleute (Stahleisen, Düsseldorf, 1995).
22. A. Ono, "Fe–Mg partitioning between spinel and olivine," J. Japan Assoc. Min. Petr. Econ. Geol. **78**, 115–122 (1983).
23. G. G. Mikhailov, L. A. Makrovets, and L. A. Smirnov, "Thermodynamic simulation of the interaction processes of lanthanum with components of iron-base metallic melts," Izv. Vyssh. Uchebn. Zaved., Chern. Met. **58** (12), 877–883 (2015).
24. G. G. Mikhailov and D. A. Zherebtsov, "On the interaction of calcium and oxygen in liquid iron," Mater. Sci. Forum **843**, 52–61 (2016). doi: 10.4028/www.scientific.net/MSF.843.52
25. T. Fuwa and J. Chipman, "The carbon–oxygen equilibria in liquid iron," Trans. AIME **218**, 887–891 (1960).
26. N. Satoh, T. Taniguchi, S. Mishima, et al., "Prediction of nonmetallic inclusion formation in Fe–40 mass % Ni–5 mass % Cr alloy production process," Tetsu-to-Hagané **95** (12), 827–836 (2009).
27. J. H. Park and H. Todoroki, "Control of $MgO \cdot Al_2O_3$ spinel inclusions in stainless steels," ISIJ Intern. **50** (10), 1333–1346 (2010). https://doi.org/10.2355/isijinternational.50.1333
28. H. Itoh, M. Hino, and S. Ban-Ya, "Thermodynamics on the formation of non-metallic inclusion of spinel ($MgO \cdot Al_2O_3$) in liquid steel," Tetsu-to-Hagané **84** (2), 85–90 (1998).
29. *Steelmaking Data Sourcebook. Japan Society for the Promotion of Science. The 19th Committee on Steelmakin*g (Gordon & Breach, New York, 1988).
30. L. J. Wang, Y. Q. Liu, Q. Wang, et al., "Evolution mechanisms of $MgO \cdot Al_2O_3$ inclusions by cerium in spring steel used in fasteners of high-speed railway," ISIJ Intern. **55** (5), 970–975 (2015).
31. H. Prox, M. Hino, and S. Ban-Ya, "Assessment of Al deoxidation equilibrium in liquid iron." Tetsu-to-Hagané **83** (12), 773–778 (1997).
32. G. K. Sigworth and J. f. Elliott, "The thermodynamics of liquid dilute iron alloys," Metal Science **8**, 298–310 (1974).
33. Yu. V. Balkovoi, P. A. Aleev, and V. K. Bakanov, *First-Order Interaction Parameters in Iron-Based Melts: Review* (Chermetinformatsiya, Moscow, 1987).
34. T. Kimura and H. Suito, "Calculation deoxidation equilibrium in liquid iron," Metall. Mater. Trans. B. **25** (1), 33–42 (1994). https://doi.org/10.1007/BF02663176
35. T. Zhang, Y. Min, C. Liu, et al., "Effect of Mg addition on the evolution of inclusions in Al–Ca deoxidized melts," ISIJ Intern. **55** (8), 1541–1548 (2015). https://doi.org/10.2355/isijinternational.ISIJINT-2014-691
36. V. I. Yavoiskii, *Theory of Steelmaking Process*es (Metallurgiya, Moscow, 1967).

Translated by Yu. Ryzhkov